Automatic Detection of MEO Satellite Streaks from Single Long Exposure Astronomic Images

Keywords: space surveillance; streak detection; medium earth orbit satellites; Radon transform.

Abstract: Nowadays, there is an increased interest in achieving an accurate surveillance of the sky, since the number of objects in Earth's orbit (active satellites and debris) is continuously increasing. The satellites constantly need to be supervised in order to notice their deviations from their trajectories and update their coordinates. This paper presents a new method for satellite detection in 2D astronomic images acquired with a cheap, easy to set up optical surveillance system. The proposed method use the Radon Transform in order to identify satellite strikes in images followed by a set of decision rules to decide whether the streak is a satellite or not. The method was tested on multiple datasets, and was found to have a very high detection rate, along with a very low false positive rate.

1 INTRODUCTION

The Earth orbits are populated by an increasing number of functional and non-functional space objects. We refer to debris as the man-made non-functional space objects and to active satellites as the functional space objects. Because of this increase of space debris, there is a real need for sky surveillance in order to monitoring either the satellites or the non-functional space objects for different purposes, such as to correct the satellites deviations from their trajectories, to detect un-cataloged space debris objects and to avoid possible collisions. Therefore, the space debris population has been extensively studied during the last decade and several surveillance systems based on radars or optical devices were developed for sky surveillance. Radar systems are mostly used for low orbit surveillance for object detection and tracking, while for orbits greater than 20000 km, the optical systems are preferred since they have a better detection rate to power requirement ratio. A detailed survey on optical solutions for space debris observations is presented in (Schildknecht, 2007).

In this paper we concentrate our attention on satellite detection for the medium earth orbits (MEO) using a cheap optical survey system. According to (Capderou, 2005), MEOs are classified as orbits with altitudes around 20000 km, while the Low Earth Orbits (LEOs) are bellow 2000 km and Geostationary Earth Orbits (GEOs) are around 36000 km from the ground. The satellites found in the MEO space are generally part of Global Navigation Satellite Systems (GNSS) (Klinkrad, 2002) such as:

- GPS (Global Positioning System) USA, U.S. Department of Defence, complete operational system, orbit major axis of 26578 km (20200 km from Earth's surface) , 6 orbital planes, 4 satellites on each orbit, orbital inclination of 55º.
- GLONASS Russia, Russian Space Forces and Ministry of Defense of the Russian Federation, complete operational system, orbit major axis of 25510 km, 3 orbital planes, a total number of 21 satellites, and orbital inclination of 45 º. (Each satellite operates in circular 19,100 km orbits at an inclination angle of 64.8 degrees and each satellite completes an orbit in approximately 11 hours 15 minutes.)
- GALILEO European Union – ESA (European Space Agency), with only 3 operational satellites per orbit, major axis of the orbit of 29600 km, 3 orbital planes, a total number of 30 satellites and orbit inclination of 56º.

Few studies exist in literature for satellites streaks detection in astronomic images, since this topic is relatively new. A first method for streaks detection was proposed in (Wallace, 2007). This method takes a first step to estimate the background noise, followed by a step where all the objects above the estimated noise are determined. Image moments

are then used to discriminate the streaks from the point-like objects that usually correspond to stars.

Levesque et al. present several contributions in (Lévesque, 2007), (Lévesque, 2009), with relevant results. Their work employs multiple techniques for background modeling and removing, for star detection and for streak detection using oriented filters.

Another more recent approach was presented in (Oniga, 2011) for LEO satellites detection in sequences of images. This work was extended in (Danescu, 2012) with a technique for measuring their 3D position in an Earth-bound coordinate system. The background (including the stars) is estimated based on previous frames in the sequence. Then the streaks are detected in the difference image between current frame and estimated background, by classifying the resulted objects based on their characteristics such as: area, major axis length, minor axis length, eccentricity, equivalent diameter, perimeter and solidity. Two identical observation systems are used, the satellite streaks are detected in each of the images, and epipolar geometry based stereovision is employed for 3D position estimation.

Motivated by the applicative importance of this topic, we introduce in this paper a new and robust approach for the detection of MEO satellite streaks. The proposed method is able to detect satellites streaks using only intensity information from a 2D image, helping thus detection in early stages within an observation sequence. This method can be further sped up by using additional cues, such as stereo information, predictions of the satellite position in the upcoming frames of the sequence and others.

The structure of this paper is as follows. In Section 2 we present the proposed method along the details of the theoretical background. Some tests and results are presented in Section 3. The paper concludes with Section 4 where some conclusions and future work lines are discussed.

2 PROPOSED METHOD

In this section we describe the proposed method for MEO satellites detection in astronomic images. Figure 1 presents the block diagram that summarizes our method. First, sequences of images are *acquired* with our own optical system. The *satellite streak detection* is then performed independently in each obtained image. For a higher precision, the input image is split into several fixed size *sub-images* (or *image windows*). A list of *satellite candidates* is generated for each image window based on the Radon transform for linear features detection. *The validation of the candidates* is then made by means of an original metric. The results of all the sub-images are then combined and a *final image* is generated, in which the detected satellites are marked in green.

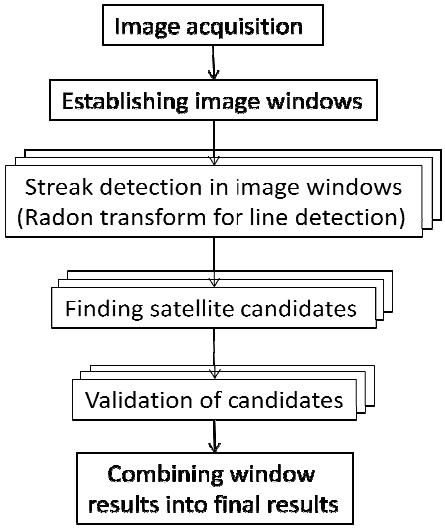

Figure 1: Block diagram.

All the mentioned steps are further detailed in the following sections. We begin by describing the astronomic optical system and the image acquisition protocol in order to better understand the addressed problem.

2.1 Image acquisition

The image acquisition system consists of two optical sensors that are placed in two different locations at a physical distance of 37 km. Each sensor has the following components:

- Newtonian 150mm, f/5 telescopes (D=150mm, F=750mm),
- DSLR Canon EOS 50D (2352 x 1568 pixels) camera, (9.4 μm x 9.4 μm) pixel size
- Equatorial tracking mount, type Celestron CG5.
- GPS based trigger for acquisition synchronization.

The acquisition is performed simultaneously with the two sensors at a exposure time of 5 seconds and the time between two frames of 8 seconds. The angular field of view of the optical system is approximately 1.5 degrees.

Due to the equatorial tracking mount with which the system is equipped, the stars are tracked during the exposure time of the acquisition process, offering thus the advantage of a relatively fixed background. Since the exposure time takes several

seconds, the MEO moving objects will be the only objects that will appear in image as a line segment. We will refer them as *satellites streaks*. The typical speed of a MEO satellite is known to be 3.9 km/s. Therefore, for an average altitude of 20000 km, the satellite will appear in the acquired images as a line segment of an approximate length of 78 pixels. Satellite length will however vary according to its altitude, angle of observation, possible variation of brightness due to its own rotation movement, etc. An example of image is provided in Fig. 2, where the satellite is indicated by the red arrow.

Figure 2: Example of MEO object (Glonass 733).

2.2 Streak detection in image windows

Having defined the main characteristics of the satellites appearance in our sequences of images, we look forward to identify the line segments of a certain length in images. The idea was to exploit the 'line segment' appearance of the satellite's streaks, which is the main feature in this type of images, and use powerful image processing techniques for line detection such as Hough transform or Radon transform to identify them.

Because the Hough transform is designed for a reduced amount of points of interest, usually obtained through thresholding, we choose instead to use the Radon transform in order to increase the detection chances for faint satellites.

More, because the satellite streaks are relatively small with respect to the image size, we choose to process smaller image windows and then recombine the results to obtain the final results.

The theoretical background of the Radon transform is described in the following sub-section.

2.2.1 Radon transform for line detection

The Radon transform is a feature extraction technique designed to solve the problem of finding parametric shapes (such as lines) through a voting procedure. Radon transform problem was first studied by Johann Radon in (Radon, 1917) in a general form and then by Deans in (Deans, 1983) who defined it the way it is used nowadays in computer vision domain, along with some of applications.

Given a 2D image I, and denoting by (x,y) the image coordinates for an image point, according to (Deans, 1983) the Radon transform is the mapping between the image space and a parametric space defined by the line integral (projections) of I along all possible lines L in the image plane. In order to obtain a bounded parametric space, the line equation is considered to be expressed in the normal form:

(1)

where represent the distance from the origin to the line, and is the angle of the vector from the origin to the closest point on the line, as illustrated in Fig. 3.

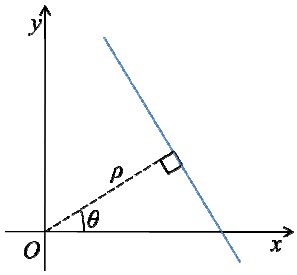

Figure 3: Line parameterization in the normal form.

Therefore, the definition of the parametric space equivalent R of the image I, for all combinations of the parameters ρ and θ, is as follows:

(2)

where ds is an increment of length along line L. Each position in the parametric space will sum up the votes for the line L of parameters as the sum of the line intensities in image space. The object candidates are then found among the local maxima in the parametric space. Knowing that the satellite streaks have high intensity with respect to (w.r.t.) the dark background (representing the night sky), high values should be assigned in parametric space for the satellite line.

Still, because the length of the satellite streak is very small w.r.t. image size, and because the astronomic images also contain many stars which have high intensities in the long exposure image (very often much higher than the satellite), finding the satellite related local maximum in a Radon transform for the entire image is impossible. For this reason, we propose to apply the Radon transform on smaller image windows and then recombine all the processing results in order to obtain the final result.

a) Searching windows: 733 (left) and PRN08 (right) satellites.

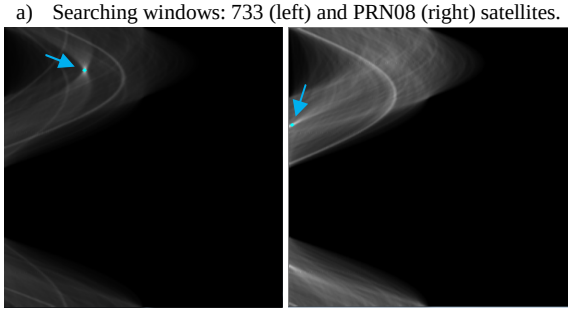

b) The corresponding parametric space. (the local maximum with highest intensity is marked with a cyan dot)

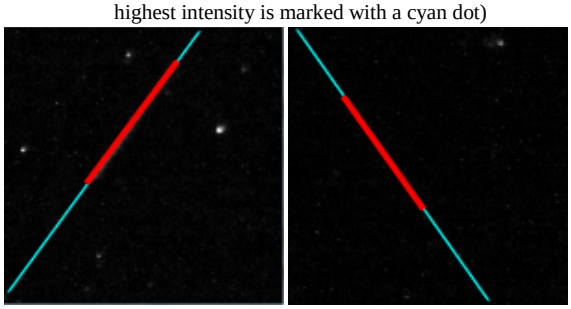

c) The image lines corresponding to the local maximum (in cyan) and the detected (satellite in red)

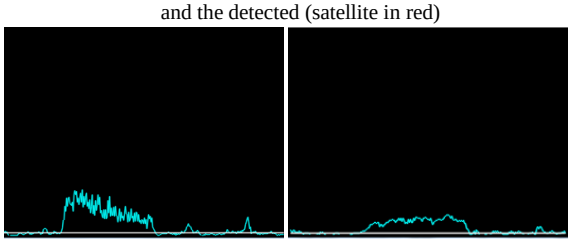

d) Plot of the cyan line intensities (from fig. c))

Figure 4: Example of searching window containing satellite streaks.

Fig. 4 shows some examples of visual result of such image windows in the first row for the Glonass 733 (left) and GPS- PRN08 (right) satellites and the corresponding parametric space obtained based on Radon transform in the second row.

An example image window that does not contain a satellite streak and its corresponding parametric space equivalent are shown in Fig. 5.

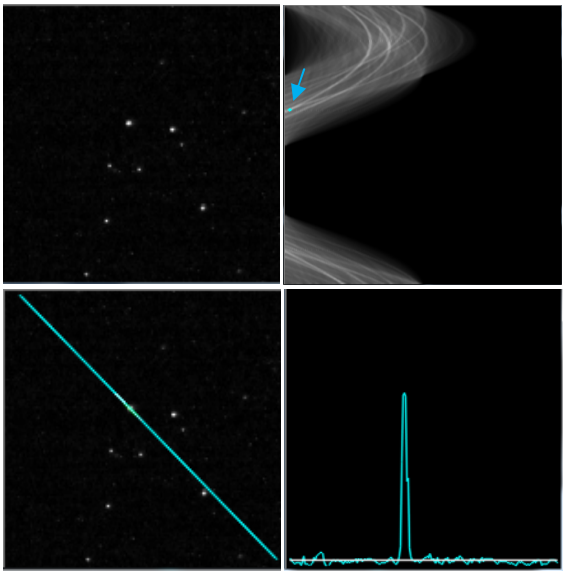

Figure 5: Example of a searching window without any satellite streaks and its corresponding parametric space.

2.3 Finding satellite candidates

The Radon parametric space is further processed in order to establish the satellite candidates. A list L_w of local maxima is generated for each image window w:

$$L_w = \{(\rho,\theta) | H(\rho,\theta) \geq H(\rho+i,\theta+j), \quad i,j = \{-1,0,1\}\}, \qquad (3)$$

Our choice of processing relatively small image windows is a strong enough constraint that imposes the fact that, if the satellite exists, it will correspond to the local maxima with the highest intensity in the parametric space. But, in order to treat the exceptional case when more satellites might occur in a single image window (which is however not the case for our dataset), we choose to consider as satellite candidates the first three local maxima with the highest votes in the parametric space. A visual example of the local maximum with the highest vote

in parametric space is displayed in Fig. 4. b) (marked by a cyan dot) and its corresponding reconstructed line in the image space in Fig. 4. b).

2.4 Validation of candidates

At this point, each image window has three candidates given as pairs of parameters (ρ, θ) in the parameter space. In order to validate the candidates, we define the following metric.

Proposed metric. For a given candidate (ρ, θ) in the parametric space, we reconstruct the corresponding line in the image (x, y) space and we plot the intensities of the line points:

$$L_{\rho,\theta}(i) = \{I(p_i) | p_i = (x_i, y_i), \rho = x_i \cos(\theta) + y_i \, sin(\theta)\} \quad (4)$$

as illustrated in Fig. 4 d), where $I(i)$ is the image intensity of the pixel i. It can be noticed that if this candidate corresponds to a satellite trajectory, then several consecutive line points will have higher intensity than the background value (TH_{bk}), since the observed satellites are brighter than the average night sky intensity (see Fig. 4 against Fig. 5). Thus, the definition of the proposed metric is as follows:

$$\begin{aligned} \text{Valid}(L_{\rho,\theta}) \leftarrow \exists n, m, \; & n > m, m > 0, \\ & n < length(L_{\rho,\theta}), (n - m) > TH_{length}, \\ & L_{\rho,\theta}(m) > TH_{bk}, L_{\rho,\theta}(m+1) \, TH_{bk}, \dots \\ & \dots, L_{\rho,\theta}(n) > TH_{bk} \end{aligned} \quad (5)$$

where TH_{length} is the minimum length that a satellite streak could have. Since we know that the mean length of a MEO satellite is around 78 pixels, this parameter can easily be set.

3 TESTS AND RESULTS

Tests were performed on a dataset of 294 images (image size = 2357×1568 pixels). The images were acquired simultaneously with the two mentioned cameras, meaning 147 images with each camera and two sets of images for each satellite. The followed objects in these sequences are four MEO satellites: two GLONASS (733, 738) and two GPS (PRN10, PRN08). The number of images where the satellites are visible is indicated in Table 1.

Table 1: Observed satellites in our dataset.

Satellite	*No of images*
733	31
738	28
PRN10	39
PRN08	32

For all images we use the same parameter settings, as follows:

- Image window w of fixed size 151×151 pixels and the distance between two image windows of 75 pixels, resulting around 650 overlapped searching windows per image,
- The background value TH_{bk} equals to the median intensity value of the whole image window w,
- The low boundary for the satellite length $TH_{length} = 60$ pixels.

Some visual detection results are displayed in Fig. 6 a), where the detected satellites are marked in green. Because of the high resolution of the images, we chose to display only the cropped area of interest from the original image results. Comparative tests were performed against the method proposed in (Oniga, 2011). See Fig. 6 b) for the visual results. An overall detection rate of hundred percent was obtained for our dataset, while only 80.76% was obtained with the comparative method (Oniga, 2011). Detailed statistics with the detection rate for each satellite is presented in Table 2.

Table 2: Satellite detection rate in comparison with (Oniga, 2011).

Satellite	*(Oniga, 2011)*	*Proposed method*
733	100%	100%
738	100%	100%
PRN10	69%	100%
PRN08	59%	100%

It can be noticed that our method successfully detects different types of satellites acquired with different cameras. It proved to deal well in detecting faint satellites instead the proposed method (Oniga, 2011) although proved to be more sensitive in detecting the GPS satellites which appear fainter than the GLONASS.

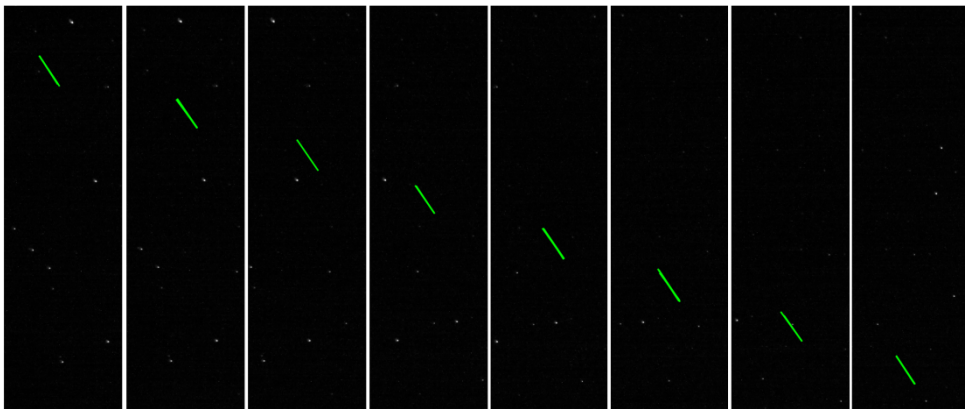

a) Proposed method. Detected object is marked in green.

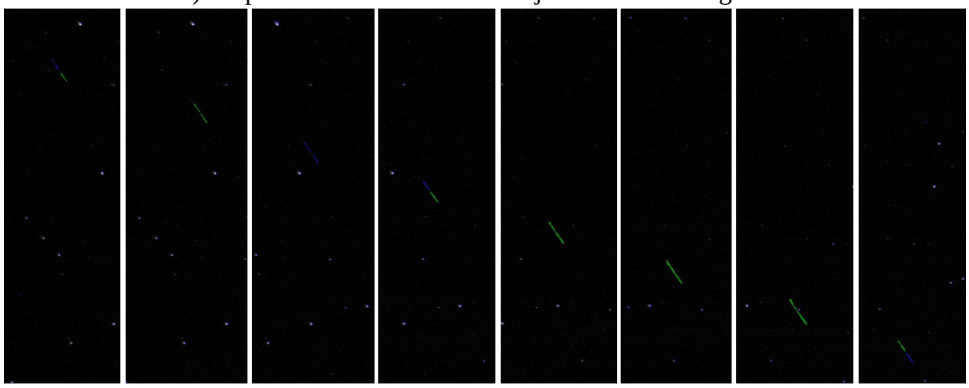

b) Comparative method (Oniga, 2011). Detected object is marked in green and other possible candidates in blue.

Fig. 6. Detection result for the GPS PRN08 in eigth consecutive frames

4 CONCLUSIONS

A new and robust method is proposed in this paper for MEO satellite detection. The central concept of the method is the use of the Radon transform on overlapping search windows, for identification of very faint linear structures. The resulted linear hypotheses are validated based on their intensity profile along the support line.

The proposed technique proves to be a high confidence MEO satellite detection solution, capable of being used even with cheap and easy to set up optical observation systems.

The method was tested for several astronomic sequences of images containing two different types of satellites and acquired with two different cameras, having different responses due to differences in location and in intrinsic capabilities of the devices. A high accuracy of 100% detection rate was obtained under all these conditions. The method robustness was also proved against a state of the art method, obtaining a higher accuracy rate and a more precise identification of the object location in image.

Additional tests need to be performed on higher and varied datasets in order to extensively validate our method.

REFERENCES

Capderou, M., *Satellites*, 2005. *Orbits and Missions*, ISBN : 2-287-21317-1, Springer-Verlag France.

Danescu, R. , Oniga, F., Turcu, V., Cristea, O., 2012. Long Baseline Stereovision for Automatic Detection and Ranging of Moving Objects in the Night Sky, *Sensors*, vol. 12, No. 10, October 2012, pp. 12940-12963.

Deans, Stanley R., 1983. *The Radon Transform and Some of Its Applications*, New York: John Wiley & Sons, 1983.

Klinkrad, H., 2002. Monitoring Space – Efforts Made by European Countries, *International Colloquium on*

Europe and Space Debris, Toulouse, France, Nov. 27-28.

Lévesque M. P., 2009. Image and processing models for satellite detection in images acquired by Space-based Surveillance-of-Space sensors, *Technical Report* no. DRDC Valcartier TR 2005-386.

Lévesque M. P., 2007. Buteau S., Image Processing Technique for Automatic Detection of Satellite Streaks, *Technical Report no. DRDC-VALCARTIER-TR*-2005-386.

Oniga, F.; Miron, M.; Danescu, R.; Nedevschi, S., 2011. Automatic recognition of low earth orbit objects from image sequences, *Intelligent Computer Communication and Processing (ICCP), IEEE International Conference on* , vol., no., pp.335-338.

Radon, Johann, 1917. Über die Bestimmung von Funktionen durch ihre Integralwerte längs gewisser Mannigfaltigkeiten, *Berichte über die Verhandlungen der Königlich-Sächsischen Akademie der Wissenschaften zu Leipzig, Mathematisch-Physische Klasse* (Leipzig: Teubner) (69): 262–277; *Translation:* Radon, J.; Parks, P.C. (translator) (1986),On the determination of functions from their integral values along certain manifolds, *IEEE Transactions on Medical Imaging* **5** (4): 170–176.

Schildknecht, T., 2007. Optical surveys for space debris. *The Astronomy and Astrophysics Review***,** *14*, 41-111.

Wallace, B., 2007. The DRDC Ottawa Space Surveillance Observatory, *AMOS Technical Conference*, Maui HI.